Phytopathology Research

RESEARCH

Open Access

Transcriptomic analysis of *Cryphonectria parasitica* during the initial infection stages reveals a glycoside hydrolase that is required for fungal pathogenicity

Xiaolin Qiu[1,2], Can Huang[1,2], Dianguang Xiong[1,2*], Lu Yu[1,2], Yuchen Yang[1,2], Xiaorong Lin[1,2] and Chengming Tian[1,2*]

Abstract

Chestnut blight, caused by *Cryphonectria parasitica*, is a notorious disease that severely harms chestnut species, leading to great economic and ecological loss worldwide. Understanding the pathogenic mechanisms of *C. parasitica* is crucial for developing effective disease control strategies. Therefore, screening and functional characterization of key pathogenic factors during *C. parasitica* and chestnut interaction are essential. Although previous studies have revealed many important virulence factors in *C. parasitica*, the underlying mechanisms need further study. Here, we examined the expression pattern of *C. parasitica* at 0, 1, 2, and 3 days post inoculation of chestnut branches (dpi) by using transcriptomic sequencing. A total of 2160 differentially expressed genes (DEGs) were identified during the infection stages compared to the uninfected control at 0 dpi. Gene ontology (GO) and Kyoto encyclopedia of genes and genomes (KEGG) analyses showed significant enrichment of upregulated genes in glycoside hydrolase activity and carbohydrate metabolism pathways. Clustering analysis revealed 66 genes that were significantly upregulated with higher fold changes during the infection process, most of which were related to the degradation of the host cell wall. Additionally, 48 putative effector genes were induced during the infection stages, which were annotated as glycoside hydrolases and chitinases as well as the hydrophobic proteins, indicating the crucial roles of glycoside hydrolase during infection processes. Subsequently, we preliminary assayed the roles of a glycoside hydrolase gene *CpEng1* and found that it was essential for fungal virulence. The results presented here provide a key resource for understanding the molecular basis of interaction between *C. parasitica* and its host.

Keywords *Cryphonectria parasitica*, Transcriptome analysis, Glycoside hydrolase, *CpEng1*, Pathogenicity

Background

Chestnut blight, first discovered in the United States in the late nineteenth century, is a notorious plant disease that causes significant damage to chestnut species worldwide (Pereira-Lorenzo et al. 2020). Filamentous fungus *Cryphonectria parasitica*, the causal agent of chestnut blight disease, penetrates and degrades host cells by physical pressure and secreting substances like oxalic acid, which disrupt normal nutrient transport, cause cankers on the chestnut bark, and ultimately lead

*Correspondence:
Dianguang Xiong
xiongdianguang@126.com
Chengming Tian
chengmt@bjfu.edu.cn
[1] State Key Laboratory of Efficient Production of Forest Resources, Beijing Forestry University, Beijing 100083, China
[2] Beijing Key Laboratory for Forest Pest Control, Beijing Forestry University, Beijing 100083, China

to the death of the whole tree (Rigling & Prospero 2017). Chestnut trees are important economic and forestry resources in many regions, the destruction caused by chestnut blight not only affects the stability of ecosystems but also significantly harms forestry economies (Ni et al. 2023). Several control measures such as cutting, burning, and spraying chemical and biological agents are commonly used (Anagnostakis 2001), but these have not been effective as anticipated. Therefore, it is necessary to systematically and thoroughly understand the molecular pathogenic mechanisms of *C. parasitica* to provide scientific and effective guidance for the control of this disease (Lovat et al. 2019).

In recent years, high-throughput sequencing technologies, particularly RNA-Seq, have rapidly progressed, providing substantial support for bioinformatics research with a wealth of sequencing data (Bliska et al. 2017). Transcriptome analysis based on high-throughput sequencing is a powerful method to comprehensively analyze gene expression patterns during the pathogenic processes with screening and identification of potential key genes, recognition of metabolic pathways, and molecular regulatory networks during the interaction (Liebhoff et al. 2023). For example, functional studies of several DEGs in *Botrytis cinerea* during the infection process through gene knockout and pathogenicity experiments demonstrated that *BcCGF1* is a new virulence-related factor that mediates fungal development and virulence by regulating spore germination, conidiation, infection structure formation, host penetration, and stress adaptation (Zhang et al. 2020). Ke et al. (2014) identified 437 DEGs during infection processes of *Valsa mali* to apple tree bark, GO and KEGG annotation showed a high frequency of genes related to pectin degradation metabolism, hydrolase activity, and biosynthesis of secondary metabolites, indicating a significant enrichment in these categories. This highlights the importance of secondary metabolites and cell wall hydrolases during the interaction between *V. mali* and apple tree.

Existing transcriptomic analysis of chestnut blight mainly focused on the interaction process between the hypovirus and *C. parasitica* or the defense mechanism of chestnut in response to the fungus infection (Barakat et al. 2012). Shang et al. (2008) constructed a mixed cDNA library of *C. parasitica* both without the virus and infected with the virus, covering both the sporulation and non-sporulation of the fungus. A cDNA microarray comprising 4845 genes, including both developmental stages, was prepared to study the changes in the gene expression profile of *C. parasitica* after infection with a low-virulence virus. The results showed that the expression levels of 1055 genes were altered, encompassing stress response, nucleic acid metabolism, and protein metabolism, and so on. This provides a new foundation for further studying the interaction between the hypovirus and its host. Chun et al. (2020) found 1023 DEGs in response to hypovirus infection to the *C. parasitica* including a large number of intracellular protein genes, indicating the alterations in specific metabolic and transport processes. Nie et al. (2023) analyzed the early defense responses of chestnut to the *C. parasitica* through RNA sequencing, and found that the fungus activated plant hormone and mitogen-activated protein kinase (MAPK) signaling pathways, plant-pathogen interaction pathways, and metabolism-related pathways in the early interaction stages. Additionally, the jasmonate (JA) biosynthesis and metabolic pathways may play an important role for the resistance of chestnut to *C. parasitica*. However, the dynamic changes of global gene expression during the different stages of *C. parasitica* and host interaction are still unclear.

As for the gene functional analyses of *C. parasitica*, several conserved virulence factors have been functionally characterized, such as the typical MAPK signaling pathway components. Deletion of *CpSte11*, a MAPKKK related to the mating and pheromone response pathway, resulted in deficiencies in growth rate, pigment formation, and fertility in *C. parasitica*. And the transcription levels of the mating pheromone precursor gene *Mf2/2* and mating response transcription factors such as *cpst12* and *pro1* were significantly downregulated in the *CpSte11* deletion mutants, indicating the crucial role of CpSte11 in the sexual mating response pathway through the downstream targets such as *cpst12*, *pro1*, and *Mf2/2* (Park et al. 2011). CpMK1, the homolog of HOG1, was required for fungal response to high osmotic stress, and its depletion led to slowed fungal growth and reduced tolerance to osmotic stress, revealing its important role in response to environmental stress in *C. parasitica* (Park et al. 2004). CpBck1 is a MAPKKK related to cell wall integrity, *CpBck1* deletion mutants exhibit phenotypic changes related to cell wall integrity, such as abnormal cell morphology and cell wall formation, severely slowed growth, and a significant reduction in fungal virulence compared to the wild type (Kim et al. 2016). Furthermore, Cplc1, encoding a specific phosphatidylinositol-specific phospholipase C (PLC), was associated with invasion of the host and pathogenicity. Research report that Cplc1 affected the production of laccase by regulating the expression of *Lac1*. Knockout of *Cplc1* resulted in slowed fungal growth and reduced virulence, indicating the crucial roles of Cplc1 in fungal growth and virulence in *C. parasitica* (Chung et al. 2006).

During the interaction between pathogens and plants, glycoside hydrolases (GHs) are crucial enzymes which can catalyze the hydrolysis of glycosidic bonds and are extensively involved in the degradation of plant cell walls,

metabolism, and signal transduction processes. Pathogens secrete these GHs to degrade plant cell walls, facilitating infection and pathogen spread. Meanwhile, plants can activate their immune responses by recognizing the secretion and activity of these GHs, thereby defending against pathogen invasion (Bradley et al. 2022). Studies have shown that GH6 and GH7 cellulases from *Magnaporthe oryzae* promote the penetration of the host epidermis (Van Vu et al. 2012); The absence of the GH10 family endo-β−1,4-xylanase VmXyl1 in *V. mali* will significantly reduce the formation of conidia and fungal virulence towards apple leaves although it not affects mycelial growth (Yu et al. 2018); The GH12 family protein XEG1, produced by the soybean pathogen *Phytophthora sojae*, exhibits xylanase and β-glucanase activities, which can also trigger plant defense responses, including plant cell death. *PsXEG1* is strongly induced during the infection processes, and both silencing and overexpression of *PsXEG1* in *P. sojae* significantly reduce its virulence. These indicate that *PsXEG1* acts as an important virulence factor during infection (Ma et al. 2015).

To systematically analyze the dynamic gene expression pattern of *C. parasitica* during infection processes, the total RNA samples of *C. parasitica* grown on the medium or after 1, 2, and 3 dpi were collected and used for subsequently sequencing. DGEs involving the pathogenicity such as cell wall degrading enzymes were identified. Among them, a glycoside hydrolase encoding gene, *CpEng1* was essential for fungal virulence. These results will increase our understanding of the pathogenic mechanism of *C. parasitica*.

Results

Transcriptome sequencing data analysis

For 12 samples collected at different times during the infection of chestnut branches by *C. parasitica*, a total of 552,224,560 raw reads were obtained from reference transcriptome sequencing. After removing adaptor sequences, N-containing sequences, and low-quality reads, 543,922,348 high-quality clean reads remained, with a filtered base count of approximately 81.59 G. The overall alignment rate on the reference genome ranged from 94.80% to 97.17%, with a Q30 between 91.03% and 92.43%, and a GC content of 57.31% to 57.91% (Additional file 1: Table S1). Consistent trends of gene expression levels and gene density were found among the samples. Heatmaps and principal component analysis (PCA) based on the Fragments per kilobase of exon model per million mapped fragments (FPKM) values of all genes in each sample were used to calculate Pearson coefficients within and between experimental groups to evaluate the reproducibility of the samples. All samples showed a squared Pearson coefficient (R^2) greater than 0.8, meeting the minimum criteria for R^2 between biologically replicated samples, and in PCA, samples were more dispersed between groups on PC1 and PC2 levels, while those within groups clustered well together, indicating a high correlation in expression patterns among the samples (Additional file 2: Figure S1).

Identification and functional annotation of differentially expressed genes

To calculate the dynamic changes of gene expression, DEGs were screened using the padj value, and the $|\mathrm{Log_2}(\text{Fold change})|$ value, which measures the degree of gene expression variation under different conditions. DEGs meeting the criteria ($\text{Padj} \leq 0.05$, $|\mathrm{Log_2}(\text{Fold change})| \geq 2$) were selected, and samples from 0 dpi, prior to infection of chestnut branches, were used as the control group. There were 1023 DEGs at 1 dpi (449 upregulated and 574 downregulated), 1363 at 2 dpi (763 upregulated and 600 downregulated), and 1682 at 3 dpi (978 upregulated and 704 downregulated). Venn diagrams revealed the overlapped genes that were consistently upregulated or downregulated across all three time points (Additional file 2: Figure S2). Among these, 298 genes were continuously upregulated during the infection stages, suggesting the putative important roles of these genes in the infection processes.

A total of 2160 DEGs were identified during the infection stages of *C. parasitica* compared to the uninfected control, which was manually divided into 18 clusters according to their expression pattern (Fig. 1). In this study, the DEGs could be separated well in the 18 clusters, which revealed a portion of specific genes that were differentially expressed with high fold change during the stages of infection. Notably, a total of 66 genes in Clusters 1 and 2 were significantly upregulated at 1 dpi, and remained steadily upregulated at 2 and 3 dpi. These DEGs with high levels of expression at the early infection stages were interesting and noteworthy. Functional annotation of these genes revealed that 15 genes were related to the degradation of the host cell wall, including glycoside hydrolases, glycosyltransferases, pectin lyases, and sugar transport proteins (Table 1), indicating their crucial role in the infection stages.

GO enrichment analysis of DEGs

To analyze the pathogenic response of *C. parasitica* during the infection process, GO annotation of DEGs at different times including biological process, cellular component, and molecular function was conducted. For each category, the top five significantly enriched GO terms were plotted in the chart (Fig. 2), which showed that the upregulated DEGs were significantly enriched in carbohydrate metabolic process and glycoside hydrolase

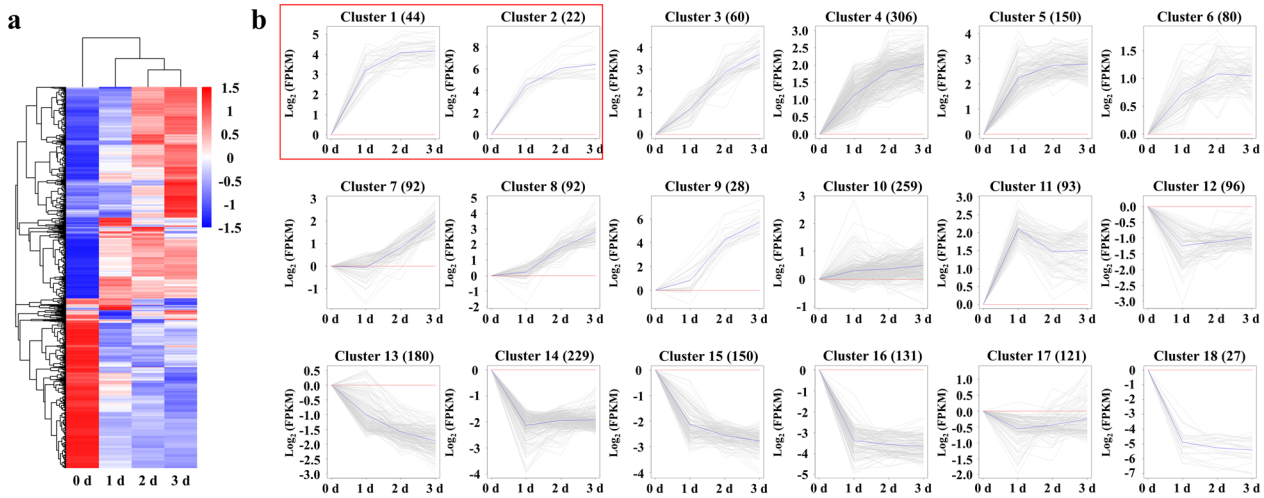

Fig. 1 Clustering of differentially expressed genes of *C. parasitica* at different infection times. **a** Heatmap is used to cluster the FPKM values of DEGs. Genes or samples with similar expression patterns are grouped together. The color in each square of the heatmap reflects the values obtained after normalizing the expression data, typically ranging between −2 and 2. **b** Trend clustering of the expression levels of all DEGs resulted in 18 distinct expression patterns. In the graph, the blue lines represent the overall expression trend of each pattern

Table 1 Functional annotation of genes related to host cell wall degradation in Cluster 1 and Cluster 2

Gene ID	Log_2(Flod change)			Gene description
	1 d vs 0 d	2 d vs 0 d	3 d vs 0 d	
Crypa1.e_gw1.1.966.1	3.455	4.220	4.096	IPR000743: Glycoside hydrolase, family 28
Crypa1.estExt_Genewise1.C_30235	3.889	6.463	6.538	IPR001223: Glycoside hydrolase family 18, catalytic domain
Crypa1.estExt_Genewise1.C_80859	2.783	4.936	5.126	IPR000757: Glycoside hydrolase family 16
Crypa1.e_gw1.4.132.1	6.896	7.819	7.446	IPR001764: Glycoside hydrolase, family 3, N-terminal IPR002772: Glycoside hydrolase family 3 C-terminal domain IPR026891: Fibronectin type III-like domain
estExt_fgenesh1_kg.C_40031	4.580	6.225	6.593	IPR003663: Sugar/inositol transporter IPR005828: Major facilitator, sugar transporter-like IPR020846: Major facilitator superfamily domain
estExt_fgenesh1_pm.C_30205	5.103	6.569	6.646	IPR003663: Sugar/inositol transporter IPR005828: Major facilitator, sugar transporter-like IPR020846: Major facilitator superfamily domain
fgenesh1_pm.7__465	3.509	4.444	3.842	IPR003663: Sugar/inositol transporter IPR005828: Major facilitator, sugar transporter-like IPR020846: Major facilitator superfamily domain
estExt_Genewise1.C_32520	3.446	3.075	4.468	IPR011701: Major facilitator superfamily IPR020846: Major facilitator superfamily domain
estExt_Genewise1Plus.C_22335	2.514	4.018	3.981	IPR011701: Major facilitator superfamily IPR020846: Major facilitator superfamily domain
estExt_Genewise1Plus.C_91757	3.637	3.392	4.484	IPR011701: Major facilitator superfamily IPR020846: Major facilitator superfamily domain
Crypa1.e_gw1.14.31.1	4.377	6.137	6.769	IPR035396: Alpha-L-rhamnosidase, six-hairpin glycosidase domain
Crypa1.fgenesh1_pg.C_scaffold_3000112	3.159	4.416	4.285	IPR045032: Pectin lyase family IPR002022: Pectate lyase
e_gw1.4.2873.1	3.158	3.412	4.047	IPR000073: Alpha/beta hydrolase fold-1
Crypa1.estExt_Genewise1Plus.C_150026	2.818	4.444	4.140	IPR003764: N-acetylglucosamine-6-phosphate deacetylase IPR006680: Amidohydrolase-related
Crypa1.fgenesh1_pg.C_scaffold_2000052	4.813	5.768	6.080	IPR004886: Glucanosyltransferase

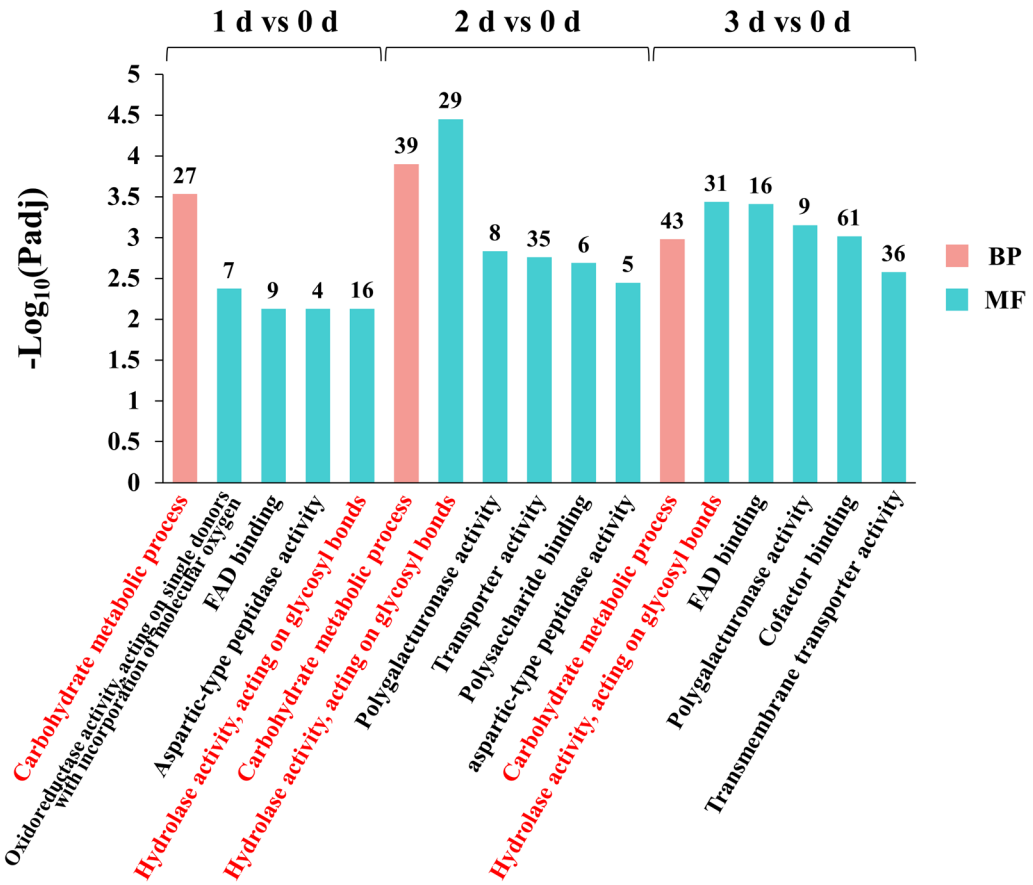

Fig. 2 GO enrichment analysis of upregulated differentially expressed genes. Bar charts are created to display the top 5 most significant terms; if there are less than 5, all terms are plotted. In the chart, the horizontal axis represents the GO term, and the vertical axis indicates the level of significance of GO term enrichment. The higher the value, the more significant it is. Different colors represent the two GO subcategories: Biological Process (BP) and Molecular Function (MF)

activity compared to 0 dpi, suggesting that degrading the host cell wall by *C. parasitica* is important for fungal infection. Additionally, downregulated DEGs were mainly focused on carboxylic acid metabolic process, oxoacid metabolic process, organic acid metabolic process, and small molecule metabolic process (Additional file 2: Figure S3). As for the cellular component cluster, most downregulated DEGs were attributed to ribosome, ribonucleoprotein complex, cytoplasm, and non-membrane-bounded organelle and the molecular function division was mainly concentrated in transferase activity, ligase activity, etc.

KEGG enrichment analysis of DEGs

To further analyze the contribution of DEGs at the metabolic pathway level, the KEGG pathway database was used for systematic classification and analysis. Upregulated DEGs were mainly enriched in the metabolic pathways of amino sugar and nucleotide sugar metabolism, pentose and glucuronate interconversions, fructose and mannose metabolism, and glycerolipid metabolism (Fig. 3). Combining with the results mentioned above, the carbohydrate metabolism pathways likely played a crucial role in the pathogenic processes of *C. parasitica* on chestnut branches. Additionally, downregulated DEGs were significantly enriched in the biosynthesis of amino acids, biosynthesis of secondary metabolites, oxalate metabolism, and the biosynthesis of valine, leucine, and isoleucine (Additional file 2: Figure S4).

Prediction of effector genes among DEGs

Effectors act as key virulence factors during the interaction between pathogens and host, which can disturb the plant immunity and trigger a series of physiological and biochemical responses. In this study, following the typical effector selection criteria, including the presence of an N-terminal signal peptide, absence of transmembrane domains, extracellular subcellular localization, lack of GPI-anchoring sites, amino acid length < 300 aa, and cysteine content ≥ 4, 48 putative effectors were

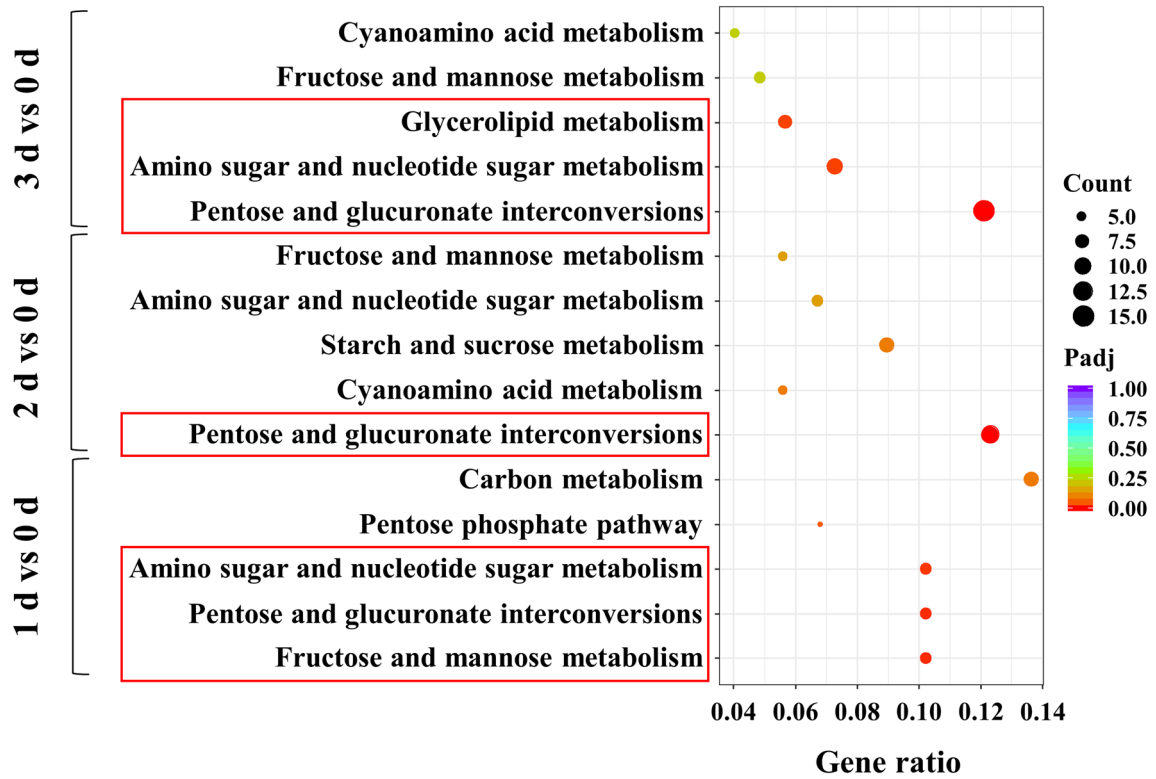

Fig. 3 KEGG enrichment analysis of upregulated differentially expressed genes. Scatter plots are created to display the top 5 most significant KEGG pathways; if there are less than 5, all pathways are plotted. In the graph, the horizontal axis represents the level of significance of pathway enrichment, and the vertical axis represents the KEGG pathways. The size of the dots indicates the number of genes annotated to each KEGG pathway. The color gradient from red to purple represents the level of significance of enrichment

predicted among the 2160 DEGs, including 29 differentially upregulated effector genes (Additional file 2: Figure S5). Among them, 16 differentially upregulated effector genes were annotated as uncharacterized proteins, and the other 13 annotated effector genes were primarily involved in the degradation of plant cell walls, including glycoside hydrolases, keratinases, chitin recognition proteins, rhamnogalacturonan acetyl esterases, and other pathogenicity-related hydrophobic proteins, phospholipases, phosphatases, and proteases.

CpEng1 is a pathogenicity-related gene in *C. parasitica*

As described above, the expression of many cell wall degradation enzyme related genes of *C. parasitica* were significantly upregulated during the infection processes, indicating their crucial roles for host infection. Among them, a dozen glycoside hydrolase genes were differentially expressed. Therefore, a glycoside hydrolase family 16 member, which encodes a putative endo-1,3(4)-β-glucanase, Crypa1.estExt_Genewise1.C_80859 (abbreviated to CpEng1), was presented in the Cluster 1 (Fig. 1), was selected for further analysis. The protein contained 287 amino acids and possessed a GH16 domain with a conserved active domain motif EXDXXE. Multiple sequence alignment analysis showed that CpEng1 had about 55% sequence identities with its homologous from other species, which are conserved among fungi. Phylogenetic analysis showed that CpEng1 in *C. parasitica* was most closely related to the homologous in *C. chrysosperma* (Fig. 4).

To reveal the function of *CpEng1* during the infection process, we used the split-marker method to knock out the *CpEng1* gene, and obtained two deletion mutants, Δ*CpEng1-49* and Δ*CpEng1-74*, which were confirmed by PCR and Southern blot analysis (Additional file 2: Figure S6b). A fragment containing the natural promoter and *CpEng1* coding sequence was isolated from *C. parasitica* genomic DNA and transformed into the Δ*CpEng1-49* mutant. *CpEng1* complemented strains were obtained through PCR screening (Additional file 2: Figure S6a). Consequently, the two mutant strains of CpEng1 (Δ*CpEng1-49*, Δ*CpEng1-74*) and one complemented strain (*CpEng1/ENG1*) were used for subsequent phenotypic analysis.

To clarify the function of *CpEng1* in the growth and development of *C. parasitica*, WT, deletion mutants,

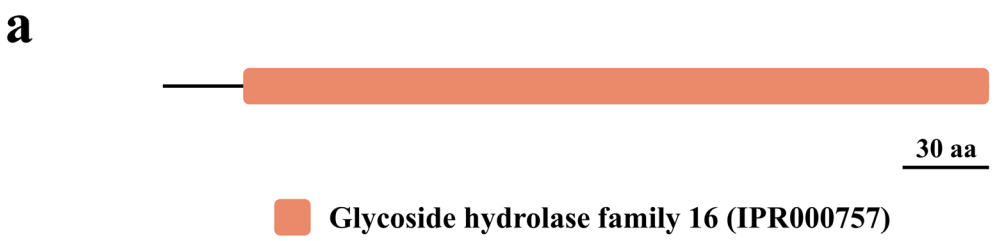

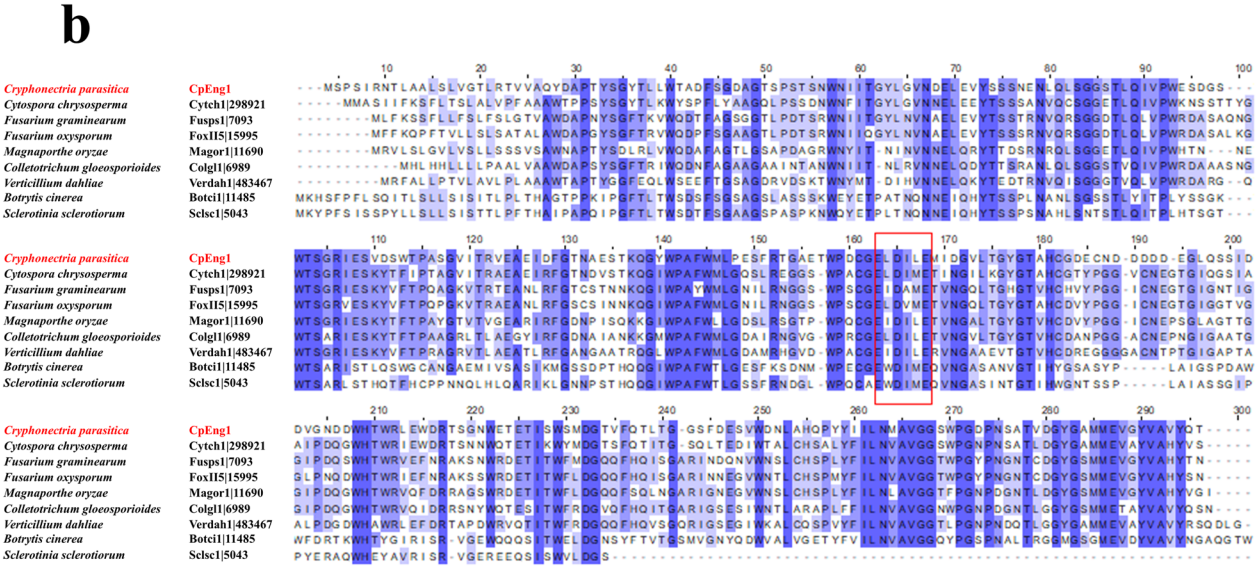

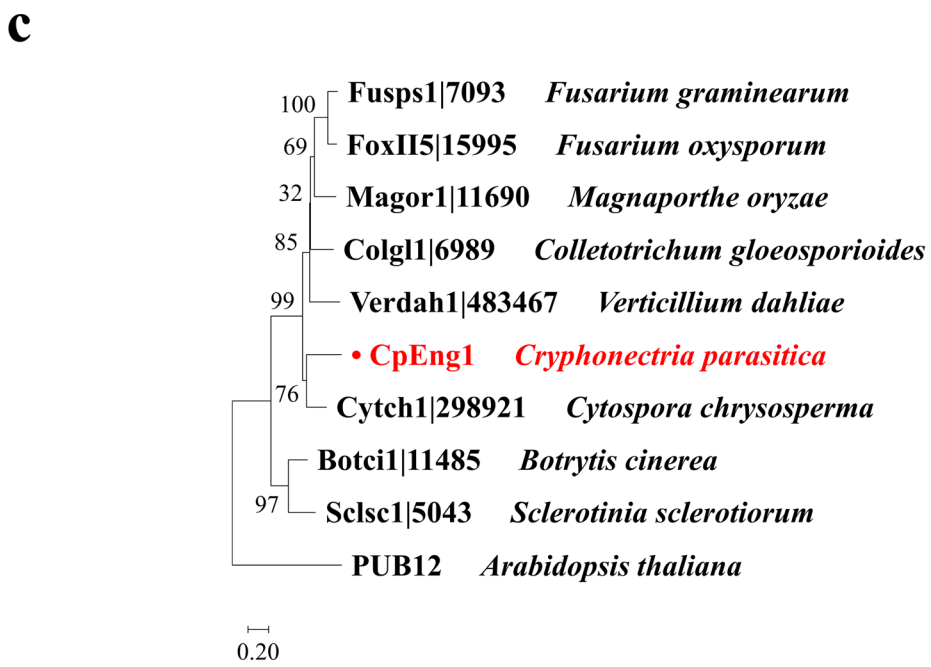

Fig. 4 Structure and phylogenetic analysis of *CpEng1*. **a** Structure of glycoside hydrolase protein CpEng1. **b** Amino acid sequence of Eng1 for *Cryphonectria parasitica* and other species (red box indicates the active structural domain feature). **c** Phylogenetic analysis of Eng1

and complemented strain were inoculated on PDA plates and observed after 24, 48, and 72 h. The results showed that the colony diameter of *CpEng1* deletion mutants was similar with that of the WT and complemented strain (Fig. 5), indicating that *CpEng1* is not essential for fungal growth and development in *C. parasitica* on artificial media.

To determine the function of *CpEng1* in the fungal virulence, WT, deletion mutants, and complemented strain were inoculated on chestnut branches. The results showed that the lesion expansion areas on branches inoculated with *CpEng1* deletion mutants was significantly smaller than those inoculated with WT and complemented strain (Fig. 6). This indicates that *CpEng1* is involved in fungal pathogenicity of *C. parasitica*.

The main components of plant cell walls include cellulose, hemicellulose, pectin, lignin, and among others. These components provide structural support and mechanical strength to the cell wall, maintaining the shape and integrity of the cell. To examine the glycoside hydrolase activity of *CpEng1* in the degradation of cell walls, WT, deletion mutants, and complemented strain were inoculated on minimal salt medium (MSM) agar plates containing glucose, cellulose, CMC-Na, laminarin, and pectin as the sole carbon source. After 20 days, the colony diameters on the MSM agar containing glucose, cellulose, and CMC-Na were essentially consistent among all strains. However, on the MSM agar supplemented with laminarin and pectin, the colony diameters of the mutant strains were significantly

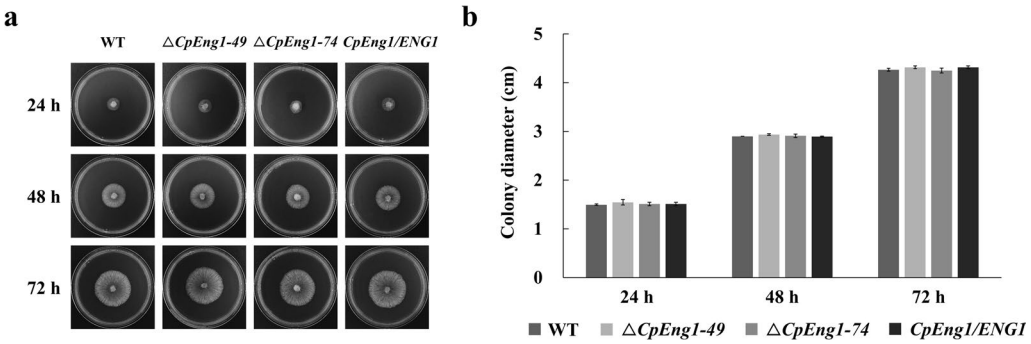

Fig. 5 Colony growth in *CpEng1* deletion mutant. **a** Colony morphologies of the WT, mutant strains, and complemented strain after 24 h, 48 h, and 72 h of growth on PDA plates. **b** Data statistics of colony diameter. Error bars are standard deviation and different lowercases represent significantly difference at $P < 0.05$

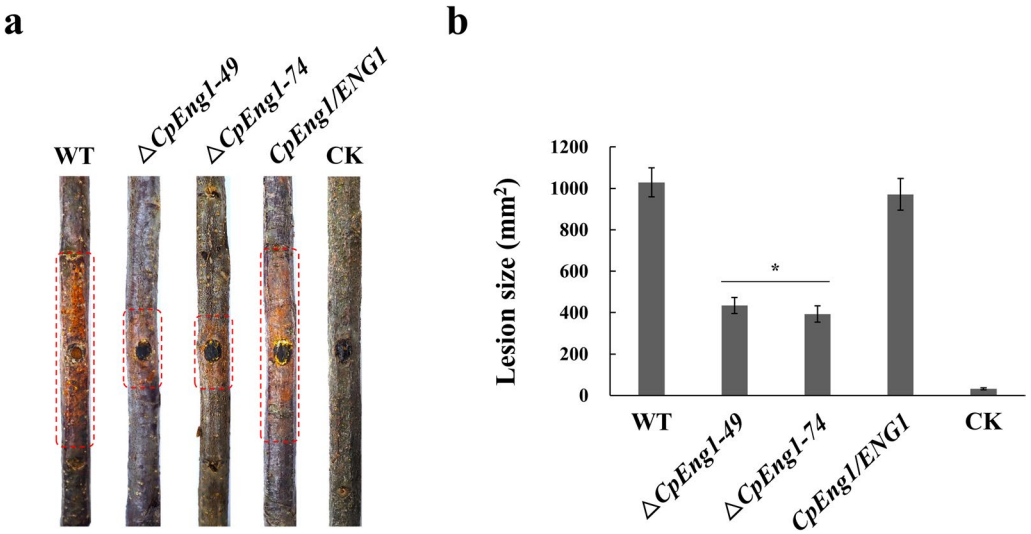

Fig. 6 Pathogenicity determination of *CpEng1* deletion mutant. **a** Spreading of lesions on detached chestnut branches inoculated with the WT, mutant strains, and complemented strain after 20 d. **b** Statistics of area of lesions on twigs. Error bars are standard deviation and different lowercases represent significantly difference at $P < 0.05$

reduced compared to the WT and complemented strain (Fig. 7), indicating that the absence of *CpEng1* affects *C. parasitica* utilization of laminarin and pectin. This suggests that *CpEng1* possesses glycoside hydrolase activity capable of degrading cell walls.

RT-qPCR validation

To validate the reliability of the RNA-seq data, eight randomly selected DEGs involved in the infection pathway were selected for RT-qPCR analysis. The qPCR expression patterns of the DEGs were found to be consistent with the RNA-seq analysis results at different stages of infestation (1 dpi, $R^2=0.9497$; 2 dpi, $R^2=0.9041$; 3 dpi, $R^2=0.8696$). It confirmed the reliability and accuracy of the RNA-seq data (Additional file 2: Figure S7a). Moreover, We showed in detail bar graphs of the differences in expression of the corresponding genes identified by RNA-seq and RT-qPCR (Additional file 2: Figure S7b).

Discussion

To further understand the transcriptional regulation characteristics of *C. parasitica* during the infection process, we conducted the transcriptome sequencing analysis of samples from 0 dpi (uninfected) as well as 1, 2, and 3 dpi, which revealed a numerous DEGs that may responsible for its pathogenicity, especially the glycoside hydrolases. Subsequently, functional analysis revealed the essential roles of a glycoside hydrolase encoding gene *CpEng1* in fungal pathogenicity.

In nature, plants utilize multiple barriers such as physical barriers, innate immunity, and physiological and biochemical mechanisms to evade pathogen infection, whereas pathogens dissolve these physical barriers and suppress the plant's innate immunity through various virulence factors to achieve successful invasion and colonization (Zhang et al. 2022). Numerous studies indicate that pathogens secrete a large amount of cell wall-degrading enzymes during the process of infecting plants, promoting pathogen invasion. Functional validation was performed on *Vmpg-3*, a pectinase from *V. mali* based on transcriptome analysis, finding that the deletion of this pectinase gene led to a decrease in pathogenicity, suggesting that *Vmpg-3* is not a decisive factor for the pathogen's virulence. The analysis suggests that other pectinases found in *V. mali* may compensate for the gene function (Ke et al. 2014). *Sclerotinia sclerotiorum* secretes numerous cell wall-degrading enzymes that damage plant cell wall components. Among these, the gene *SsXyl1*, encoding an endo-β−1,4-xylanase, shows significantly increased expression during sclerotia development and germination, as well as during the infection stage. When *SsXyl1* is knocked out, mutant strains exhibit abnormal sclerotia development and lose virulence toward the host, demonstrating the crucial role of this enzyme in the growth, colonization, and pathogenicity of *S. sclerotiorum* (Yu et al. 2016). The GH12 protein FoEG1, secreted by *Fusarium oxysporum*, acts as a pathogen-associated molecular pattern (PAMP) targeting plant intercellular spaces, inducing cell death. The expression of FoEG1 is strongly induced in the early stages of *F. oxysporum* infecting its host plants, and the absence or loss of enzymatic activity of FoEG1 weakens the virulence of *F. oxysporum*. This indicates that FoEG1 can enhance the virulence of *F. oxysporum* based on its enzymatic activity and can also serve as a PAMP to induce plant defense responses (Zhang et al. 2021). Consistently, in this study, a significant proportion of genes related to the degradation of the host cell wall were found, such as those encoding glycoside hydrolases, glycosyltransferases, and pectin lyases. GO and KEGG functional enrichment analyses

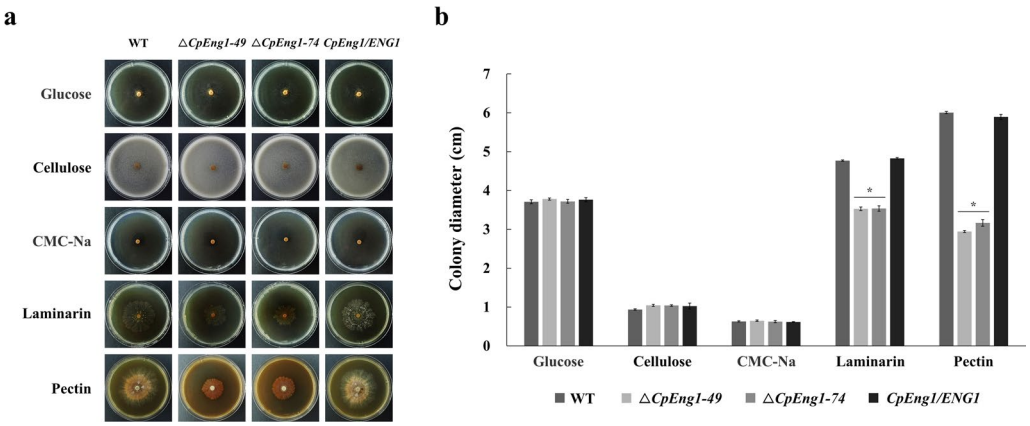

Fig. 7 *CpEng1* can degrade laminarin and pectin as carbon source. **a** After 20 days of growth on MSM agar plates supplemented with glucose, cellulose, CMC-Na, laminarin, and pectin as the sole carbon sources, the colony morphology of the WT, mutant strains, and complemented strain. **b** Data statistics of colony diameter. Error bars are standard deviation and different lowercases represent significantly difference at $P<0.05$

found that glycoside hydrolase activity and carbohydrate metabolism pathways were significantly enriched during the infection process. This study selected a GH16 family endo-1,3(4)-β-glucanase, *CpEng1*, which is significantly differentially expressed in the early stages of *C. parasitica* infection, for functional verification. It was found that *CpEng1* is not necessary for the regulation of mycelial growth and development but significantly reduces the pathogenicity of *C. parasitica* on chestnut branches, indicating that this gene is one of the key virulence factors during the infection stage of *C. parasitica*.

The glycoside hydrolase families within plant pathogens exhibit a conserved role in enzymatic activity, which are crucial for the invasion of hosts and development of disease (Kubicek et al. 2014). These enzymes are specifically designed to target the polysaccharide components of plant cell walls, such as cellulose, hemicellulose, and pectin, which can effectively degrade these complex polysaccharide structures, and then promote the infection of plant tissues (Zhao et al. 2013). The deletion of *xyn11A*, which encodes a GH11 family endo-β−1,4-xylanase, significantly affects the virulence of *B. cinerea*. When endo-β−1,4-xylanase secretion was induced with beechwood xylan, the enzyme activity was measured in culture filtrates from WT and mutant strains, revealing that the enzyme activity in the mutant decreased by approximately 30%. Additionally, the deletion of *xyn11A* affected the accumulation of reducing sugars in the medium after xylan hydrolysis, indicating that *xyn11A* has glycoside hydrolase activity (Brito et al. 2006). After culturing the CcEG1 deletion mutant and WT strains of *Cytospora chrysosperma* on a basic medium with glucose, CMC-Na, or cellulose as the sole carbon source for 5 days, it was found that the colony diameter on glucose medium was similar among the strains. However, compared to WT, the growth rate of the mutant strain on media with added CMC-Na and cellulose was significantly impaired. This suggests that the absence of CcEG1 affects cellulose utilization and validates the glycoside hydrolase activity of CcEG1 (Xu et al. 2023). The conserved activity of glycoside hydrolases not only reflects their central role in the life activities of pathogens but also indicates their high degree of homology and substrate specificity across different plant pathogen species throughout the evolutionary process. This underscores their universal importance in pathogen infection and the development of plant diseases (O'Connell et al. 2012). In this study, the GH16 family endo-1,3(4)-β-glucanase *CpEng1* of *C. parasitica*, a laminarinase, was investigated. We found the absence of *CpEng1* affects the utilization of laminarin and pectin, and the glycoside hydrolase activity of *CpEng1*, revealing the mechanism of action of the pathogen in degrading the host cell wall and the infection process. The endo-1,3(4)-β-glucanase from the GH16 family belongs to laminarinase and can specifically degrade laminarin. This specificity is due to its structural features and active sites being specially adapted to recognize specific glycosidic bonds on the substrate. Such specificity originates from the construction of the enzyme's active center, which exhibits a high degree of complementarity with the specific substrate. A total of 118 genes annotated to the glycosyl hydrolase family were found in the transcriptome of *C. parasitica* during the initial infection stages, of which 31 were differentially expressed including 23 up-regulated genes. During pathogen-host interactions, different GHs may target specific substrates or participate in specific physiological responses, and certain GHs may be activated only under specific physiological conditions or in specific tissues. Not all GHs are involved in the immune response of the plant or in the infection process of the pathogen.

Furthermore, this study identified 48 potential effector proteins within the genes that showed variable expression levels. Among these, 29 were notably upregulated. They mainly included enzymes and proteins such as glycoside hydrolases, keratinases, chitin recognition proteins, rhamnogalacturonan acetylesterases, and various hydrophobic proteins related to pathogenicity, along with phospholipases, phosphatases, proteases, etc. Additionally, the study found a significant increase in the expression of genes related to oxidoreductases in the first two clusters of DEGs trend clustering. This suggests that, beyond cell wall-degrading enzymes, hydrophobic proteins, proteases, and oxidoreductases are likely crucial for cell wall breakdown and cell death in *C. parasitica*, indicating a complex pathogenic mechanism. For instance, the aspartic protease produced by *B. cinerea* degrades the cell walls and intracellular proteins of the host carrot and participates in the formation of fungal toxins to complete infection (Movahedi et al. 1990). Moreover, some of pathogenicity-related genes of *C. parasitica* described previously such as *CpSte11*, *CpMK1*, *CpBck1,* and *Cplac1*, were significantly up-regulated during the initial infection stages. Their important roles in the pathogenicity were also verified.

In this study, we conducted a comprehensive transcriptome analysis of *C. parasitica* during the infection process, which revealed a large number of DEGs. Among them, the glycoside hydrolase activity and carbohydrate metabolism were significantly enriched. Additionally, CpEng1, a significantly upregulated glycoside hydrolase, was selected for functional validation which was proved to be an important pathogenic factor for *C. parasitica*. The present results will increase our knowledge on the interactions between *C. parasitica* and chestnut.

Conclusion

This study comprehensively analyzed the transcriptome during the infection process of *C. parasitica*, revealing its gene expression patterns involved in pathogenicity. The results showed that, compared to the uninfected control group, genes related to cell wall degradation were significantly upregulated among the DEGs. GO and KEGG functional enrichment analyses indicated that genes associated with glycosyl hydrolase activity and carbohydrate metabolism were prominently expressed during the infection process. The predicted effector proteins within the DEGs were mainly glycosyl hydrolases involved in plant cell wall degradation, suggesting that breaking down the cell wall of chestnut branches is a key pathogenic strategy of the fungus. Functional validation of the pathogenicity-related virulence factor CpEng1 revealed that its deletion did not affect the vegetative growth of the pathogen but significantly reduced its pathogenicity. This study aids in elucidating the molecular mechanisms of pathogenicity in *C. parasitica* and provides novel insights for the effective control of chestnut blight in the future.

Methods

Fungal strains and cultivation conditions

The WT strain of *C. parasitica* used for transcriptome sequencing in this study was originated from the Forest Pathology Laboratory of Beijing Forestry University. The WT strain of *C. parasitica* EP155 (ATCC 38755) used for gene knockout and functional analyses was kindly provided by professor Baoshan Chen from Guangxi University (Crouch et al. 2020). All fungal strains used in this study were regularly cultured on potato dextrose agar medium (PDA; 20% potato extract, 2% glucose, and 1.5% agar) at 25 °C. For DNA and RNA extraction, mycelia were cultured in liquid potato dextrose broth medium (PDB; 20% potato extract and 2% glucose) for 2 days at 150 rpm, 25 °C.

Sample preparation for RNA-Seq analysis

To prepare the transcriptome sequencing samples, the isolated chestnut branches were cut into 5 cm long branch segments, rinsed with distilled water, and sterilised with 1% sodium hypochlorite, then rinsed clean with sterile water and air-dried. Some of the branches were ring peeled to remove the bark, and they were scalded with a soldering iron. A small clump of freshly grown mycelium, approximately 1 cm in diameter and cultured in PDB liquid medium for 2 days, was inoculated onto the burn site, which was then wrapped in bark to increase the contact area between the mycelium and scalded wounds. The inoculated branches were placed in petri dishes lined with moistened filter paper and covered with cling film and placed at 25 °C for incubation. Mycelia were collected at 0 dpi directly from PDB liquid media and 1, 2, 3 dpi from chestnut branches, rapidly frozen in liquid nitrogen, ground into powder, and total RNA was extracted from the powder using the RNA Easy Fast Plant Tissue Kit (TIANGEN, China) according to the manufacturer's protocol. RNA quality was checked on 1% agarose gels, with each time point samples being replicated three times.

Transcription sequencing and bioinformatic analysis

After detecting RNA integrity and concentration using agarose gel electrophoresis and Agilent 2100 bioanalyzer, the sequencing libraries were generated using the NEBNext Ultra RNA Library Prep Kit for Illumina (NEB, USA) according to the manufacturer's recommendations. The libraries were sequenced on an Illumina HiSeq platform and 150 bp paired-end reads were generated. The paired-end clean reads were aligned to the reference genome using Hisat2 v. 2.0.5 (Kim et al. 2019). Differential expression analysis was performed using the DESeq2 R package v. 1.16.1 (Love et al. 2014). The resulting p values were adjusted using Benjamini and Hochberg's approach for controlling the false discovery rate. Genes with an adjusted $p < 0.05$ found by DESeq2 were assigned as differentially expressed. GO and KEGG enrichment analyses of differentially expressed genes were performed using the clusterProfiler R package. GO terms with corrected $p < 0.05$ were considered significantly enriched by differentially expressed genes.

The putative effectors of *C. parasitica* were predicted based on the following criteria: presence of an N-terminal signal peptide, absence of transmembrane domains, extracellular subcellular localization, absence of GPI-anchoring sites, amino acid length < 300 aa, and cysteine residues ≥ 4. SignalP-5.0 (https://services.healthtech.dtu.dk/services/SignalP-5.0/) was used to predict the signal peptides of effectors, DeepTMHMM-1.0.24 (https://dtu.biolib.com/DeepTMHMM) was used for predicting transmembrane domains, TargetP-2.0 (https://services.healthtech.dtu.dk/services/TargetP-2.0/) was used for subcellular localization, and big-PI Predictor (http://mendel.imp.ac.at/gpi/fungi_server.html) was used for for GPI-anchoring sites (Lovelace et al. 2023).

Sequence and phylogenetic analysis

The sequence of *CpEng1* was acquired from *C. parasitica* EP155 genome database in the JGI database (https://mycocosm.jgi.doe.gov/Crypa2/Crypa2.home.html). Structural domains were identified using the Interpro database (http://www.ebi.ac.uk/interpro/). Blastp searches were performed on national center for

biotechnology information (NCBI, https://www.ncbi.nlm.nih.gov/) and joint genome institute (JGI, https://mycocosm.jgi.doe.gov/mycocosm/home) to find homologous proteins of CpEng1 in other pathogens. Protein sequence alignment was conducted using the online ClustalW tool (https://www.genome.jp/tools-bin/clustalw), and visualized with Jalview software. The software Mega 11.0 was used to construct a phylogenetic tree using the Neighbor-Joining method, with bootstrap analysis repeated 1000 times (Tamura et al. 2021).

Targeted gene knockout and complementation

The gene *CpEng1* was knocked out by using the split-marker approach (Goswami 2012). The mycelia of *C. parasitica* were enzymatically digested with 20 mL enzyme solutions consisting of 0.25 g Driselase, 0.2 g Lysozyme, and 0.2 g Cellulase to produce protoplasts. A PEG-mediated genetic transformation system was employed to introduce the constructed homologous recombination fragments into the protoplasts of *C. parasitica*. The transformants were firstly grown on TB_3 solid medium containing 25 mg/L hygromycin and then covered by PDA solid medium with 30 mg/L hygromycin. The obtained transformants were cultured at 25 °C for 3—5 days to DNA extraction. PCR amplification and Southern blot analysis were conducted using primers External-CpEng1for/External-CpEng1rev and Internal-CpEng1for/Internal-CpEng1rev to determine the successfully single copy recombination mutants.

The full-length complementation fragment, including the *CpEng1* promoter and entire coding region PCR was amplified with primers CpEng1-Compfor/CpEng1-Comprev. This full-length complementation fragment, along with the geneticin (G418) resistance gene, was co-transformed into the protoplasts of the Δ*CpEng1-49* strain. The transformants were grown in TB_3 solid medium containing 25 mg/L hygromycin and 60 mg/L G418, followed by selection on PDA solid medium with 30 mg/L hygromycin and 75 mg/L G418. PCR amplification and screening of the complemented transformants were conducted using primers Internal-CpEng1for/Internal-CpEng1rev. All primers used in this study are listed in Additional file 1: Table S2.

Fungal growth assays

Mycelial plugs with a diameter of 5 mm were taken from PDA plates of the WT, deletion mutants, and complemented strains after incubation at 25 °C for 48 h. These plugs were inoculated onto new PDA plates and incubated at 25 °C for 24, 48, and 72 h. The colony diameters were then measured. Each experiment was replicated at least three times.

Pathogenicity assays

Fresh chestnut branches were collected and cut into 30 cm segments, rinsed with distilled water, disinfected with 1% sodium hypochlorite, and then washed with sterile water. The upper ends of the branches were sealed with paraffin. A 5 mm diameter iron circle was heated and used to scorch the branches. Mycelial plugs of 5 mm diameter from PDA plates of WT, deletion mutants, and complemented strains were then inoculated on the scorched areas of the branches and secured with sealing film. The inoculated branches were maintained at room temperature with high humidity for 20 d, after which observations and photographic records were taken. The lesion area was covered with a transparent film, and the edges of the lesion were traced on the film with a pen. The lesion area was then calculated using the grid counting method, and each strain was replicated three times in the experiment.

Enzyme activity measurement

The glycoside hydrolase activity of *C. parasitica* was assessed using the plate colony growth rate method. Glucose, cellulose, CMC-Na, laminarin, and pectin were added to the MSM (purchased from Beijing Coolaber, http://www.coolaber.com/), each making a 20 g/L specific carbon source MSM. After incubating WT, deletion mutants, and complemented strain on PDA plates at 25 °C for 48 h, mycelial plugs with a diameter of 5 mm were inoculated on the above-mentioned specific carbon source MSM plates. After incubating at 25 °C for 20 days, the colony diameters were measured. Each experiment was replicated at least three times.

Validation of DEGs by RT-qPCR

To confrm the reliability of the data obtained by RNA-seq, eight genes associated with pathogenicity in DEGs including Crypa1.estExt_Genewise1.C_30235, Crypa1.e_gw1.4.132.1, Crypa1.e_gw1.1.966.1, estExt_Genewise1.C_52594, Crypa1.estExt_fgenesh1_pg.C_110177, Crypa1.e_gw1.9.156.1, estExt_Genewise1Plus.C_91757, and estExt_fgenesh1_pm.C_90282 were randomly selected for RT-qPCR validation. The primers used in this experiment are listed in Additional file 1: Table S2. RNA was reverse transcribed into cDNA using a Hifair III 1st Strand cDNA Synthesis SuperMix for qPCR (Yeasen, China) and real-time PCR was performed using a Hieff UNICON Universal Blue qPCR SYBR Green Master Mix (Yeasen, China). Each sample was established with three replicates and the *CpActin* gene of *C. parasitica* was used as the reference. All data represent the standard deviation of three biological replicates.

Statistical analysis

All data were exhibited as mean value ± standard error, the mean and the standard deviations was derived from three independent biological replicates with three technical replicates each. All statistical analyses were performed with one-way ANOVA followed by Duncan's range test using SPSS 22.0.

Abbreviations

dpi	Days post inoculation
DEGs	Differentially expressed genes
GO	Gene ontology
KEGG	Kyoto encyclopedia of genes and genomes
MAPK	Mitogen-activated protein kinase
JA	Jasmonate
PLC	Phospholipase C
GHs	Glycoside hydrolases
PCA	Principal component analysis
FPKM	Fragments per kilobase of exon model per million mapped fragments
MSM	Minimal salt medium
PAMP	Pathogen-associated molecular pattern
PDA	Potato dextrose agar
PDB	Potato dextrose broth
NCBI	National center for biotechnology information
JGI	Joint genome institute

Supplementary Information

The online version contains supplementary material available at https://doi.org/10.1186/s42483-025-00315-7.

Additional file 1: Table S1. Quality statistics of transcriptome sequencing of *Cryphonectria parasitica* at different infection times. **Table S2.** List of primers.

Additional file 2: Figure S1. Quantitative analysis of transcriptomic data of *C. parasitica* at different infection times. **Figure S2.** Differentially expressed genes of *C. parasitica* at different infection times. **Figure S3.** GO enrichment analysis of downregulated differentially expressed genes. **Figure S4.** KEGG enrichment analysis of downregulated differentially expressed genes. **Figure S5.** Heatmap of 29 upregulated effectors in differentially expressed genes. **Figure S6.** Targeted gene deletion and complementation. **Figure S7.** Validation of the expression of candidate genes during infection as determined by quantitative real-time RT-qPCR analysis.

Acknowledgements

We thank Prof. Baoshan Chen (Guangxi University) for kindly providing the WT strain of *C. parasitica* EP155 (ATCC 38755).

Author contributions

CT and DX initiated, coordinated, and supervised the project. XQ, YY, and XL conducted the experiments and gathered the data. XQ, LY, and CH analyzed the data and drafted the manuscript. XQ, CT, DX, and LY reviewed and revised the manuscript. All authors read and approved the fnal version of the manuscript.

Funding

This work was supported by the National Key Research and Development Program (2023YFD1401301).

Availability of data and materials

Not applicable.

Declarations

Ethics approval and consent to participate

Not applicable.

Consent for publication

Not applicable.

Competing interests

The authors declare that they have no competing interests.

Received: 14 May 2024 Accepted: 14 January 2025
Published online: 22 April 2025

References

Anagnostakis SL. American chestnut sprout survival with biological control of the chestnut-blight fungus population. ForEst Ecol Manag. 2001;152:225–33.

Barakat A, Staton M, Cheng C-H, Park J, Yassin N, Ficklin S, Sederoff R. Chestnut resistance to the blight disease: insights from transcriptome analysis. BMC Plant Biol. 2012;12:38.

Bliska JB, Westermann AJ, Barquist L, Vogel J. Resolving host–pathogen interactions by dual RNA-seq. PLoS Pathog. 2017;13: e1006033.

Bradley EL, Ökmen B, Doehlemann G, Henrissat B, Bradshaw RE, Mesarich CH. Secreted glycoside hydrolase proteins as effectors and invasion patterns of plant-associated fungi and oomycetes. Front Plant Sci. 2022;13: 853106.

Brito N, Espino JJ, González C. The endo-beta-1,4-xylanase xyn11A is required for virulence in *Botrytis cinerea*. Mol Plant Microbe Interact. 2006;19:25–32.

Chun J, Ko Y-H, Kim D-H. Transcriptome Analysis of *Cryphonectria parasitica* Infected With Cryphonectria hypovirus 1 (CHV1) Reveals Distinct Genes Related to Fungal Metabolites, Virulence, Antiviral RNA-Silencing, and Their Regulation. Front Microbiol. 2020;11:1711.

Chung H-J, Kim M-J, Lim J-Y, Park S-M, Cha B-J, Kim Y-H, Kim D-H. A gene encoding phosphatidyl inositol-specific phospholipase C from *Cryphonectria parasitica* modulates the lac1 expression. Fungal Genet Biol. 2006;43:326–36.

Crouch JA, Dawe A, Aerts A, Barry K, Churchill ACL, Grimwood J, Nuss DL. Genome sequence of the chestnut blight fungus *Cryphonectria parasitica* EP155: a fundamental resource for an archetypical invasive plant pathogen. Phytopathology. 2020;110:1180–8.

Goswami RS. Targeted gene replacement in fungi using a split-marker approach. Methods Mol Biol. 2012;835:255–69.

Ke X, Yin Z, Song N, Dai Q, Voegele RT, Liu Y, Huang L. Transcriptome profiling to identify genes involved in pathogenicity of *Valsa mali* on apple tree. Fungal Genet Biol. 2014;68:31–8.

Kim J-M, Lee J-G, Yun S-H, So K-K, Ko Y-H, Kim YH, Kim D-H. A Mutant of the Bck1 Homolog from *Cryphonectria parasitica* Resulted in Sectorization with an Impaired Pathogenicity. Mol Plant-Microbe Interact. 2016;29:268–76.

Kim D, Paggi JM, Park C, Bennett C, Salzberg SL. Graph-based genome alignment and genotyping with HISAT2 and HISAT-genotype. Nat Biotechnol. 2019;37:907–15.

Kubicek CP, Starr TL, Glass NL. Plant cell wall-degrading enzymes and their secretion in plant-pathogenic fungi. Annu Rev Phytopathol. 2014;52:427–51.

Liebhoff A-M, Menden K, Laschtowitz A, Franke A, Schramm C, Bonn S. Pathogen detection in RNA-seq data with Pathonoia. BMC Bioinformatics. 2023;24:53.

Lovat CA, Donnelly DJ, Doğmuş-Lehtijärvi HT. Mechanisms and metabolomics of the host–pathogen interactions between Chestnut (Castanea species) and Chestnut blight (*Cryphonectria parasitica*). Forest Pathol. 2019;49: e12562.

Love MI, Huber W, Anders S. Moderated estimation of fold change and dispersion for RNA-seq data with DESeq2. Genome Biol. 2014;15:550.

Lovelace AH, Dorhmi S, Hulin MT, Li Y, Mansfield JW, Ma W. Effector Identification in Plant Pathogens. Phytopathology. 2023;113:637–50.

Ma Z, Song T, Zhu L, Ye W, Wang Y, Shao Y, Wang Y. A *Phytophthora sojae* Glycoside Hydrolase 12 Protein Is a Major Virulence Factor during Soybean Infection and Is Recognized as a PAMP. Plant Cell. 2015;27:2057–72.
Movahedi S, Heale JJP, Pathology MP. Purification and characterization of an aspartic proteinase secreted by *Botrytis cinerea* Pers ex. Pers in culture and in infected carrots. Physiol Mol Plant Pathol. 1990;36:289–302.
Ni C, Liu Y, Liu Y, Li H, Shi M, Zhang M, Han B. First Report of Chestnut Blight Caused by *Cryphonectria parasitica* on Chestnut (Castanea seguinii) in Gansu Province. China Plant Disease. 2023;107:942.
Nie X, Zhao S, Hao Y, Gu S, Zhang Y, Qi B, Qin L. Transcriptome analysis reveals key genes involved in the resistance to *Cryphonectria parasitica* during early disease development in Chinese chestnut. BMC Plant Biol. 2023;23:79.
O'connell RJ, Thon MR, Hacquard S, Amyotte SG, Kleemann J, Torres MF, Vaillancourt LJ. Lifestyle transitions in plant pathogenic Colletotrichum fungi deciphered by genome and transcriptome analyses. Nat Genet. 2012;44:1060–5.
Park SM, Choi ES, Kim MJ, Cha BJ, Yang MS, Kim DH. Characterization of HOG1 homologue, CpMK1, from *Cryphonectria parasitica* and evidence for hypovirus-mediated perturbation of its phosphorylation in response to hypertonic stress. Mol Microbiol. 2004;51:1267–77.
Park JA, Kim JM, Park SM, Kim DH. Characterization of CpSte11, a MAPKKK gene of *Cryphonectria parasitica*, and initial evidence of its involvement in the pheromone response pathway. Mol Plant Pathol. 2011;13:240–50.
Pereira-Lorenzo S, Bischofberger Y, Conedera M, Piattini P, Crovadore J, Chablais R, Lefort F. Reservoir of the European chestnut diversity in Switzerland. Biodiv Conserv. 2020;29:2217–34.
Rigling D, Prospero S. *Cryphonectria parasitica*, the causal agent of chestnut blight: invasion history, population biology and disease control. Mol Plant Pathol. 2017;19:7–20.
Shang J, Wu X, Lan X, Fan Y, Dong H, Deng Y, Chen B. Large-scale expressed sequence tag analysis for the chestnut blight fungus *Cryphonectria parasitica*. Fungal Genet Biol. 2008;45:319–27.
Tamura K, Stecher G, Kumar S. MEGA11: molecular evolutionary genetics analysis version 11. Mol Biol Evol. 2021;38:3022–7.
Van Vu B, Itoh K, Nguyen QB, Tosa Y, Nakayashiki H. Cellulases belonging to glycoside hydrolase families 6 and 7 contribute to the virulence of *Magnaporthe oryzae*. Mol Plant Microbe Interact. 2012;25:1135–41.
Xu Z, Luo Z, Xiong D, Gao M, Tian C. A glycoside hydrolase 12 protein from *Cytospora chrysosperma* triggers plant immunity but is not essential to virulence. Phytopathol Res. 2023;5:1–15.
Yu Y, Xiao J, Du J, Yang Y, Bi C, Qing L. Disruption of the Gene Encoding Endo-β-1, 4-Xylanase Affects the Growth and Virulence of *Sclerotinia sclerotiorum*. Front Microbiol. 2016;7:1787.
Yu C, Li T, Shi X, Saleem M, Li B, Liang W, Wang C. Deletion of Endo-β-1,4-Xylanase VmXyl1 Impacts the Virulence of *Valsa mali* in Apple Tree. Front Plant Sci. 2018;9:663.
Zhang MZ, Sun CH, Liu Y, Feng HQ, Chang HW, Cao SN, Qin QM. Transcriptome analysis and functional validation reveal a novel gene, BcCGF1, that enhances fungal virulence by promoting infection-related development and host penetration. Mol Plant Pathol. 2020;21:834–53.
Zhang L, Yan J, Fu Z, Shi W, Ninkuu V, Li G, Zeng H. FoEG1, a secreted glycoside hydrolase family 12 protein from *Fusarium oxysporum*, triggers cell death and modulates plant immunity. Mol Plant Pathol. 2021;22:522–38.
Zhang S, Li C, Si J, Han Z, Chen D. Action mechanisms of effectors in plant-pathogen interaction. Int J Mol Sci. 2022;23:6758.
Zhao Z, Liu H, Wang C, Xu JR. Comparative analysis of fungal genomes reveals different plant cell wall degrading capacity in fungi. BMC Genomics. 2013;14:274.